Hindawi
Mobile Information Systems
Volume 2022, Article ID 9157150, 9 pages
https://doi.org/10.1155/2022/9157150

Research Article

Rapid Restoration of Medical Images Relying on Bayesian Personalized Sorting Algorithm

Yuanhao Cao

School of Information Engineering, North China University of Water Resources and Electric Power, Zhengzhou 450046, Henan, China

Correspondence should be addressed to Yuanhao Cao; caoyuanhao@ncwu.edu.cn

Received 25 March 2022; Revised 29 April 2022; Accepted 16 May 2022; Published 22 June 2022

Academic Editor: Hafiz Tayyab Rauf

Aiming at the real-time problem of medical image depth information restoration, which leads to the incomplete image data information collected in the process of medical image data acquisition, this study proposes a fast medical image restoration method based on the Bayesian personalized sorting algorithm (BPSA), which is used to segment the low- and high-frequency sub-band images in the initial image, The optimal low-frequency sub-band coefficient is solved by combining the nonnegative matrix decomposition method, and the high-frequency direction sub-band coefficient is solved according to the local contrast of the image and the energy in some regions, to obtain the characteristics of the medical image. The medical image information can be quickly restored by triangulation, which solves the disadvantages of too many image feature points and long operation time in the traditional image restoration method. Finally, the experimental research shows that the medical image fast restoration method proposed in this study has a better effect on texture detail restoration, which can effectively reduce the time of medical image depth information restoration and can also effectively improve the accuracy, which shows the effectiveness and practicability of the algorithm.

1. Introduction

At present, the storage of personal data is required in e-government medical and health care and other information systems. Personal data have been easier to use. However, those stored in systems are at the risk of misuse by operators/system admins. Thus, the prevention and control techniques have been developed as required [1, 2]. How to reuse the transferred data and save patient information in a personalized structure is one of the tough issues to be addressed in the storage of image data. Electronic imaging systems need to store patient information for a long time, which can be obtained at any time. However, considering the limited life of computer hardware and database capacity, data cannot be stored online for a long time. The distorted data information is restored and reused to ensure that the relevant data information of the patient's medical database can be stored in the system, to ensure that the difficulties encountered in the storage process of medical image data can be solved. At present, the rapid restoration of medical images in China will continue to implement image restoration. With the continuous deepening of medical reform, it has become an important mode for optimizing the healthcare service model and will also become the target of the country's key development of the health industry, which can meet the needs of home users to the greatest extent [3, 4]. It can effectively improve the utilization efficiency of medical and health resources and continuously enhance the effective management and control of rapid medical image restoration, thereby comprehensively and effectively improving the interaction ability of image restoration level of rapid medical image restoration. As a current image restoration system, the optimization of rapid medical image restoration method can effectively simplify the manual management process while continuously digitizing the system, which can effectively illustrate the advancement of heuristic optimization of rapid medical image restoration methods, and finally complete the unified deployment and step-by-step implementation of

image restoration. The basis of the optimization of the fast medical image restoration method is the user information resources, and the user resource information and management and control efficiency will be crucial for optimizing the fast medical image restoration method. Therefore, the rapid restoration of medical images requires full analysis and reasonable management and control of user information data. The optimization of the medical image fast restoration method is the optimization of the traditional medical image fast restoration problem. It is mainly for users to receive services at one or more image restoration points [5,6]. However, the medical image fast restoration is mainly based on the perspective of the public. In the process of image restoration, the problem of restoration path planning is solved according to the patient's condition. In the process of image restoration, the restoration path planning problem is usually solved according to the patient's condition. Fast image restoration is carried out for traditional fast restoration problems of medical image, to use the Bayesian personalized sorting algorithm to optimize fast medical image restoration under image restoration, considering that the planning problem of fast medical image restoration method usually occurs in the whole process of image restoration; however, the difference between home nursing service and hospital nursing service is that the main focus of home nursing is that the caregiver is not limited by working hours, while the constraints of hospital restoration generally consider time and capital investment. This optimization of the fast medical image restoration method can be used to realize the image restoration service, which can effectively solve this problem [7–9]. As the development basis of these imaging technologies, computer and medical image processing technology are driving the profound reform of modern medical diagnosis. The clinical application of various new medical imaging methods has made great progress in medical diagnosis and treatment technology. At the same time, the information obtained by various imaging technologies is complementary, which also provides a strong scientific basis for clinical diagnosis and biomedical research. Therefore, medical image processing technology has been highly valued by relevant experts at home and abroad. Through the Bayesian personalized sorting algorithm data, with regard to the phenomenon of high packet loss rate in the image restoration implementation causing the Bayesian personalized sorting algorithm data loss, the Bayesian personalized sorting algorithm image restoration implementation method is used, to make up the missing data to ensure the safe realization of fast restoration data of medical image. A computer network is an important part of the image archiving and communication system. It is responsible for providing the underlying image transmission service. It is the software and hardware basis of the image archiving and communication system. It is through various levels of networks that the image acquisition, storage and display, medical data management, and other units in the image archiving and communication system are connected together to form a unified and high-performance system. PACS needs to solve the problems of data transmission and image storage. Using limited storage space to save more images has become the key of compression space technology.

Aiming at the increasing demand for rapid medical image restoration and many problems exposed in the current development of image processing, this study combines the Bayesian personalized sorting algorithm with the medical image rapid restoration method to achieve the image restoration on the basis of fully analyzing the reasons, which is mainly divided into two stages: the upper layer and the bottom layer for fast rapid restoring. By making detailed planning for the decision-making stage of the medical image fast restoration method in the upper layer and using the Bayesian personalized sorting algorithm in the bottom layer image fast restoration stage, it can make the user complete the search for the largest space within the specified time. It can be observed from the final results of the experiment that the proposed algorithm can optimize the rapid restoration method for medical images and implement the function of image restoration.

2. Bayesian Personalized Sorting Algorithm

In the Bayesian personalized sorting algorithm, the acquired image data are mainly used to define the pattern value points as probability density f(x), maximum value, and probability density, and zero is taken as the value using the gradient $\nabla f(x)$. Thus, the kernel function of the probability density at the point x for n sampled points $\{x_i | i = 1, \ldots, n\}$ in the d-dimensional space can be expressed as follows:

$$\widehat{f}(x) = \frac{1}{nh^d} \sum_{i=1}^{n} K\left(\frac{x_i - x}{h}\right). \tag{1}$$

In the above equation, K(x) is a kernel function $K(x) = k(\|x\|^2)$. It is defined that g(x) = -k′(x) and $G(x) = k(\|x\|^2)$, and the mean shift vector at the point x is defined as follows:

$$M_{h,G}(x) = \frac{\sum_{i=1}^{n} G\left(x_i - x/h\right)\left(x_i - x\right)}{\sum_{i=1}^{n} G\left(x_i - x/h\right)}. \tag{2}$$

It is assumed a given original point $x = y$, the kernel function is $G(x)$, and the expression (3) is executed repeatedly until it reaches and remains in a state of convergence. Thus, the pattern value points can be obtained, as described as follows:

$$y_{i-1} = \frac{\sum_{i=1}^{n} G\left(x_i - y_j/h\right)x_i}{\sum_{i=1}^{n} G\left(x_i - y_j/h\right)}. \tag{3}$$

The image data adopted mainly contain spatial information and color features. In accordance with the selected sample database X, it complies with $d = p + 2$ ($p = 1$ indicates grayscale space, and $p = 3$ indicates color images). Subsequently, based on the image space obtained, the corresponding image feature vector can be expressed by $X = [x^s, x^r]^T$. Thus, the spatial coordinates of the image are denoted by x^s, and the color features of the image are denoted by x^r. Since there is a certain connection between the size of the space where the image is located and the size of

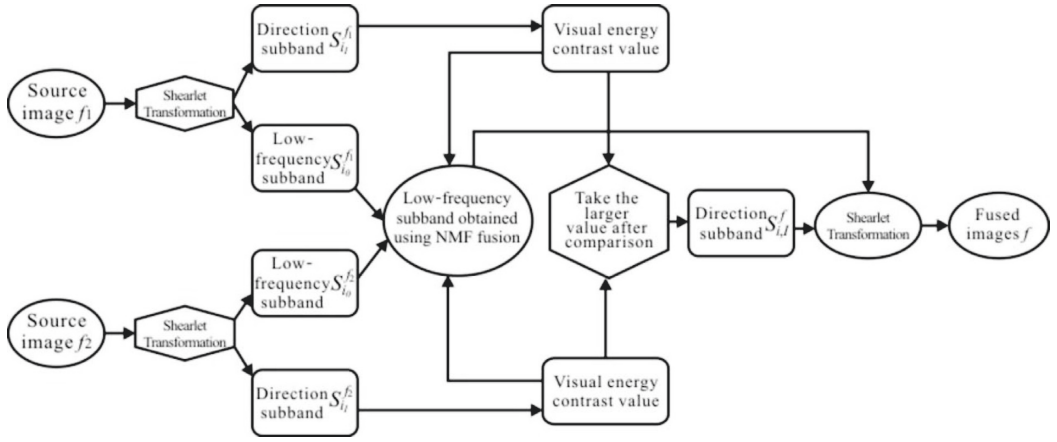

Figure 1: Block diagram of the Bayesian personalized sorting algorithm.

the phase in the color space, the kernel function used can be expressed by two spatial kernel functions, as shown as follows:

$$G(x) = G_s(x^s)G_r(x^r). \tag{4}$$

The original image is denoted by x_i, and the image after being smoothed is denoted by $z_i\,(i = 1, \cdots, n)$, separately. In addition, the image is smoothed based on the mean shift method. For each pixel point, the following is carried out:

(1) $j = 1$ is initialized, and let $y_{i,1} = x_i$.

(2) The center at the current position within the spatial bandwidth h_s is computed, in which h_s stands for the spatial bandwidth and h_r stands for the color bandwidth.

$$y_{i,j+1} = \frac{\sum_{k=1}^{m} x_k g\left(\left\|y_{i,j}^s - x_k^s/h_s\right\|^2\right) g\left(\left\|y_{i,j}^r - x_k^r/h_r\right\|^2\right)}{\sum_{k=1}^{m} g\left(\left\|y_{i,j}^s - x_k^s/h_s\right\|^2\right) g\left(\left\|y_{i,j}^r - x_k^r/h_r\right\|^2\right)}. \tag{5}$$

(3) $m_G(y_{i,j}) = y_{i,j+1} - y_{i,j}$.

(4) Step 2 to step 3 are repeated until $\|m_G(y_{i,j})\| < \varepsilon$, and the convergence point $z_i^r = y_{i,c}$ can be obtained.

(5) The value $z_i = (x_i^s, y_{i,c}^r)$ is assigned.

In this study, the Bayesian personalized sorting algorithm is used to complete the rapid repair of low-frequency sub-band coefficients, and the low-frequency sub-band coefficients after rapid repair $S_{i_0}^f$ are obtained; for the rapid repair of high-frequency direction sub-band coefficients, the visual energy contrast method is used to complete, and the high-frequency direction sub-band coefficients after rapid repair $S_{i,l}^f$ are obtained; finally, through the Shearlet inverse operation, the rapid repair image is obtained. The flow of the rapid repair algorithm proposed in this study is shown in Figure 1.

Firstly, a Bayesian personalized sorting algorithm is performed on the original image after strict registration, and the original image is broken down into $|\text{slope}_A(x_{iA}, y_{iA}) - \text{slope}_B(x_{iB}, y_{iB})| \le \theta_d$ (a low-frequency sub-band) and θ_d (high-frequency sub-band series) represented by the coefficients of the Bayesian personalized sorting algorithm, where $c = 1, 2, \ldots, N$, stands for the cth high-frequency sub-band of the image, $k = 1, 2, \ldots, M$ (i, j) is the decomposition direction parameter, which stands for the position of the Bayesian personalized sorting algorithm coefficient in the direction to break down the images in multiple directions at multiple scales. Subsequently, the coefficients of low- and high-frequency sub-bands are rapidly restored, and then, an inverse operation is performed to get the final rapid restoration image [10–12]. The specific decomposition steps of the Bayesian personalized sorting algorithm are as follows:

(1) The original image is decomposed into images of various scales T_0, T_1, …, $T_{N,}$ through non-down-sampling tower decomposition…, where T_0 stands for the decomposed coarse-scale image, and T_1~T_N represents the decomposed 1st subdivision scale image to the Nth subdivision scale image.

(2) Through the rapid two-dimensional Fourier transform, the subdivision scale images T_1, …, T_N transform to frequency domain FT_1, …, FT_N.

(3) Each subdivision scale frequency domain image FT_1, …, FT_N is used as the input of the Bayesian personalized sorting algorithm filter bank $\theta_d = \pi/8$, through the multi-directional decomposition of (x_{iA}, y_{iA}), and the frequency domain coefficients (x_{iB}, y_{iB}) of each high-frequency sub-band are obtained. A series of high-frequency sub-band coefficients $\{a_1, a_2, a_3, \ldots, a_{N_A}\}$ are obtained through the rapid two-dimensional inverse Fourier transform of $\{b_1, b_2, b_3, \ldots, b_{N_B}\}$.

(4) Based on the result T_0 of step 2, $S_0(i, j) = T_0$ is directly made, and the result $a'_{k+l} = a_{k+i} - (1/n)\sum_{j=0}^{n-1} a_{k+j}$ of step 4 is synthesized, and then, all the coefficients of the Bayesian personalized sorting algorithm are obtained.

(5) The coefficients of low- and high-frequency sub-bands corresponding to the decomposed source image are rapidly restored according to a specific rapid restoration algorithm, and the coefficients of

low- and high-frequency sub-bands of the rapid restoration image are obtained, respectively.

(6) Through the personalized sorting function, the rapid restored image is obtained.

3. Rapid Restoration Process of Medical Image

3.1. Rapid Restoring Algorithm Flow. For the purpose of obtaining continuous edges of the image, through the association of the image edge pixels with the image in the central region, it is assumed that a breakpoint between two edge segments A and B can be obtained. However, for the endpoint (x_{iA}, y_{iA}) of the image edge A in the neighborhood of the endpoint (x_{iB}, y_{iB}) of the edge B, it can be argued that the edges of the aforesaid image can be merged into one edge. The k-slope where the endpoint (x_{iA}, y_{iA}) of the image edge A is located is calculated, which can be described using the following expression:

$$\text{slope}_A(x_{iA}, y_{iA}) = \arctan\left(\frac{y_{iA+k} - y_{iA}}{x_{iA+k} - x_{iA}}\right). \tag{6}$$

In the above expression, (x_{iA+k}, y_{iA+k}) stands for the kth point under the image edge A with the endpoint (x_{iA}, y_{iA}) as the starting point, in which k is usually a relatively small value (e.g., $k = 4$). It is assumed that $|\text{slope}_A(x_{iA}, y_{iA}) - \text{slope}_B(x_{iB}, y_{iB})| \le \theta_d$ (in which θ_d stands for the threshold value, such as $\theta_d = \pi/8$), and then, the endpoints (x_{iA}, y_{iA}) and (x_{iB}, y_{iB}) of the two edges A and B of the image can be connected by a straight-line segment to form an edge.

With regard to the fast repair of open edges, we apply the improved chain code representation method from the literature. For the two open edges A and B repaired quickly, the corresponding improved chain code representations are first calculated. It is assumed that the improved chain codes for the two fast repair objects of open edges A and B come from the two open edges with the length of n (in general, n is greater than 2/3 of the minimum length of the open edges A and B) [13–16]. With regard to the fragment α and fragment β of $\{a_1, a_2, a_3, \ldots, a_{N_A}\}\{b_1, b_2, b_3, \ldots, b_{N_B}\}$, α starts from the kth edge point of A, and β starts from the first edge point of B. Thus, the fast repair degree between α and β can be defined as follows:

$$D_{kl}^{n} = \frac{1}{n}\sum_{j=0}^{n-1} \cos\frac{\pi}{4}\left(a'_{k+j} - b'_{l+j}\right). \tag{7}$$

In the above equation, $a'_{k+l} = a_{k+i} - (1/n)\sum_{j=0}^{n-1} a_{k+j}$ and $b'_{k+l} = b_{k+i} - (1/n)\sum_{j=0}^{n-1} b_{k+j}$, $0 \le i < n$. Subsequently, the optimal fast repair pair $(K_n, L_n) = \arg\max_{kl}(D_{kl}^{n})$ is identified when the slice length is n, and its fast repair degree is denoted as $D_{K_nL_n}^{n}$.

It is assumed that for different two images of the closed edges A and B corresponding to the closed regions of R_A and R_B, the first six moment invariants of their corresponding seven moment invariants are calculated based on the traditional algorithm due to the moment invariants, which are denoted as $\{\phi_{iA}', i = 1, 2, \ldots, 6\}$ and $\{\phi_{iB}', i = 1, 2, \ldots, 6\}$, respectively. Then, the six invariant moment function equations are normalized, as shown as follows:

$$\phi_i' = \frac{\phi_i}{\sqrt{\sum_{i=1}^{6} \phi_i^2}}. \tag{8}$$

Subsequently, the following is calculated as follows:

$$d_{AB} = \sqrt{\sum_{i=1}^{6} \left[\phi_{iA}' - \phi_{iB}'\right]^2}. \tag{9}$$

If d_{AB} is less than a certain threshold value d (a smaller value of d indicates more stringent requirement for the degree of rapid repair of the two edges. In general, $d = \sqrt{\sum_{i=1}^{6} [\phi_{iA}' + \phi_{iB}'/2]^2} \times 5\%$ can be taken; that is, the two closed edges A and B are considered as closed edges for rapid repair.

For the purpose of obtaining sufficient closed edges, the quick repair-to-open edges into closed edges are converted in this study by connecting the two endpoints of the edges that are quickly repaired to the open state into straight-line segments to form closed edges. The specific process is shown in Figure 2. Figure 2(a) shows a fast-repaired open edge, in which the two endpoints of the opening are connected via a straight-line segment. In this way, the fast-repaired closed edge in Figure 2 can be obtained, as shown in Figure 2(b).

3.2. Rapid Restoration Rules for High-Frequency Sub-Band Coefficients. The Bayesian personalized sorting algorithm is centered on medical images with medical image storage and control as the core. Many medical images will be created with the advent and rapid progress of wireless communications supported by massive terminals in the society. There is no doubt that great attention will be paid to medical image storage and control. For this purpose, a Bayesian personalized sorting algorithm-based scheme for the storage of medical images is proposed. This study introduces the Bayesian personalized sorting algorithm technology to carry out the design of the Bayesian personalized sorting algorithm-based storage system for the huge quantity of medical images to implement their storage intelligently and ensure information service security. A rapid restoration management system of medical images is established by consolidating the doctor-nurse-patient management, and the system is compared and analyzed before and after its launch, and simulation experiments are carried out.

The fast repair function module of high-frequency sub-band coefficient is mainly used to ensure that the color and spatial size of each image pixel reconstructed can be restored to the initial color and characteristics of the image to a certain extent. The repair function used for the fast repair of the high-frequency sub-band coefficient adopts the L^{inp} representation. In accordance with the repair of the unmasked image, the degree of damage to the masked image area, the damage due to usage, and the image confrontation can be expressed in the equation as follows:

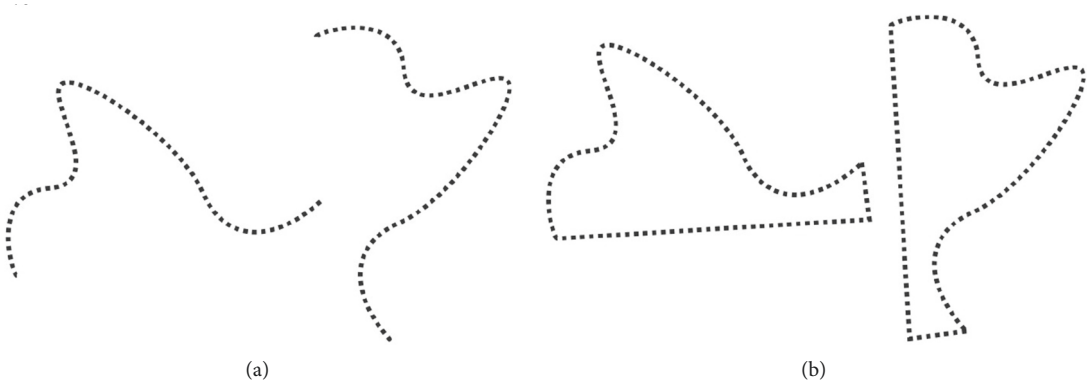

(a) (b)

Figure 2: Schematic diagram of converting open edges into closed ones. (a) Matched open contour pair. (b) Closed contour pair after conversion.

$$L_{\text{total}}^{\text{inp}} = 2L_{\text{valid}} + 12L_{\text{hole}} + 0.04L_{\text{per}} + 100\left(L_{\text{style}}^{1} + L_{\text{style}}^{2}\right). \tag{10}$$

According to the expression for the repair of image damage described above, the repaired medical image with the actual image corresponding to the non-masked image area that can be used for the repair of the damaged image is expressed in (9) as follows. In the expression, I_{dam} stands for the medical image that has yet to be repaired, M stands for irregular binary mask, I_{dam} stands for the repaired medical image, and I_{inp} stands for the actual unused algorithm under the repaired medical image. Thus, the expression of the restoration loss function for the masked region can be obtained as follows:

$$\begin{aligned} L_{\text{valid}} &= \left\| M \times \left(I_{\text{inp}} - I_{\text{dam}}\right) \right\|_1, \\ L_{\text{hole}} &= \left\| (1 - M) \times \left(I_{\text{inp}} - I_{\text{dam}}\right) \right\|_1. \end{aligned} \tag{11}$$

It is worth noting that medical images still have certain limitations. The storage of medical images is an incremental process, and patients are accumulated one by one when they visit a doctor. If the circumstance of seeing a doctor occurs, the incremental update is required. However, due to hardware capacity, service life, and other factors, long-term storage of medical images is infeasible. How to store, transfer effectively, and use personal medical images is an essential issue worth careful study. For the sharing of medical images, patients visit different medical institutions, and the forms and writing habits of different institutions are different. How to use it effectively and comprehensively is also an urgent issue to be addressed. With regard to the medical image security, medical images contain many physiological and other personal privacy issues. This information is easily leaked. Meanwhile, the information transmission process has some security risks. This study uses the characteristics of human vision to obtain the detailed information contained in images and designs visual energy contrast to select the coefficients of rapidly stored images according to the characteristics of high-frequency sub-band coefficients.

With regard to the quick fix of medical images, it is defined using diversity and accuracy, and comprehensive evaluation is carried out to accomplish the quick fix of medical image selectively. Through composing medical image quick fixes in the medical image based on the particle swarms in the search space, the information feature vector χ_i of the corresponding medical image quick fix data can be expressed as follows:

$$l_{\varepsilon}(g) = (1 - \rho) l_{\varepsilon}(g - 1) + \gamma f\left(\chi_i(g)\right). \tag{12}$$

In the above expression, f stands for the adaptive function corresponding to the feature vector χ_i of the feature data in the medical image quick fix. $\gamma\chi_i(g)$ stands for the εth quick fix corresponding to the medical image quick fix in the practical application process.

The expression for the quick fix π_p in the medical image quick fix II can be obtained as follows:

$$Acu\left(\pi_p\right) = \text{NMI}\left(\pi_p, \pi^*\right). \tag{13}$$

In the above equation, π_p and π_q stand for the fast fix for the medical image. If there is less information shared with the base cluster of medical image quick fix, the accuracy of this base cluster will be relatively low; otherwise, the accuracy of this base cluster will be relatively high. On the basis of the accuracy and diversity features of the clusters for rapid medical image repair, the comprehensive evaluation criteria for defining the clusters based on rapid medical image repair can be expressed as follows:

$$\text{Eval}\left(\pi_p\right) = \lambda Acu\left(\pi_p\right) + (1 - \lambda)\text{Div}\left(\pi_p\right). \tag{14}$$

In the above equation, $\lambda \in [0, 1]$. The correctness and diversity of medical images for rapid repair stand for the degree of importance in the comprehensive assessment criteria.

4. Analysis of Experiment and Results

In this study, the simulation experiment of the Bayesian personalized sorting algorithm is realized using MATLAB simulation software on PC, and the characteristic points of medical images are obtained. During the experiment, the algorithm in this study and the SIFT algorithm were used to restore the original image rapidly, and the results were compared and analyzed, and the feature vector of medical

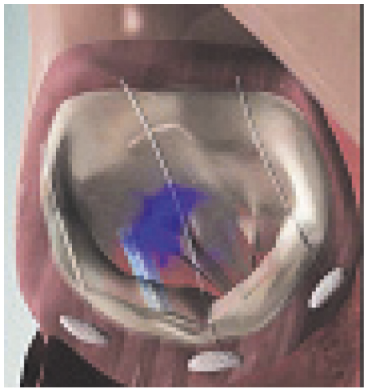

Figure 3: Left image.

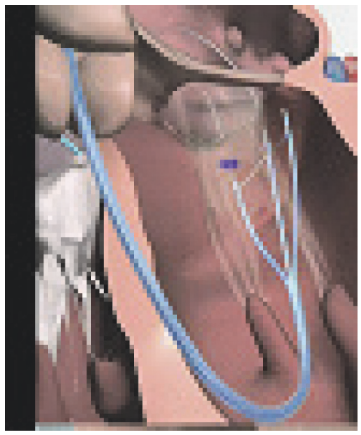

Figure 4: Right image.

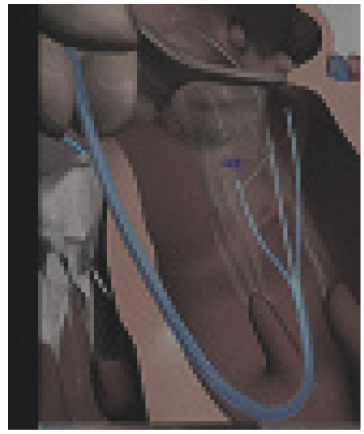

Figure 5: Image restored by SIFT algorithm.

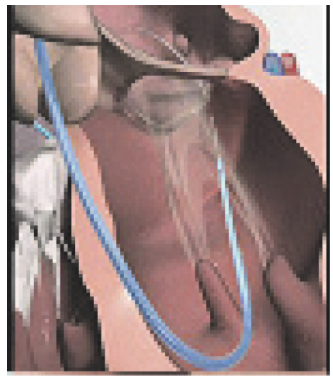

Figure 6: Restoration diagram of the Bayesian personalized sorting algorithm.

images was extracted effectively based on the Bayesian personalized sorting algorithm. The medical image restoration image of the mitral valve cable is selected as the research target to obtain the original images (Figures 3 and 4). In the image restoring process, the focal point distance selected by the camera is 0.5 m, and the threshold for rapid image restoring is set to 0.48. The image restoring results obtained using the Bayesian personalized sorting algorithm are shown in Figures 5 and 6. Among them, Table 1 shows the results of rapid image restoration in Figures 5 and 6. The above two images indicate that more feature vectors can be obtained by the Bayesian personalized sorting algorithm in the process of rapid medical image restoration than by the SIFT algorithm. It reduces the data capacity and the number of feature point images that need to be restored to a certain extent, which greatly saves the time required for rapid image restoration. Compared with the characteristics of image restoration by SIFT algorithm, on the basis of ignoring some obvious characteristics, it can effectively reduce the amount of calculation and the frequency of calculations generated in the image feature description stage, effectively improve the accuracy of image restoration, and can effectively meet the requirements of medical image processing.

With regard to the medical images with different sizes, part of the contents in a medical image can be copied and pasted to the rest of that medical image, as shown in the restored medical image 1 to the restored medical image 3 in Figure 6. The hardware platform CPU is CPU 1.5 GHz, with a memory of 725 MB, and the sizes of the chunked medical images are 30×30 pixels 20×20 pixels, and 20×20 pixels, and all the cumulative contribution rates selected for principal component extraction by CFOA are 85%. MATLAB 6.0 is used to perform programming so as to implement the neural network algorithm and the algorithm put forward in this study. In addition, the contrast of the experimental results of the medical images is represented in Figure 7.

Table 1: Rapid restoring result statistics.

Algorithm	SIFT	BPSA
Number of matching points	75	32
Number of mismatching points	4	2
Matching rate (%)	96.15	96.45
Matching time (s)	5.83	2.45

In this study, similar to the neural network algorithm, analysis can be carried out on the medical image restoration regions to indicate the effectiveness of the proposed method. It can also be observed that the analyzed restoration regions are more accurately localized. This suggests that the gray-scale information of the medical images in the neural

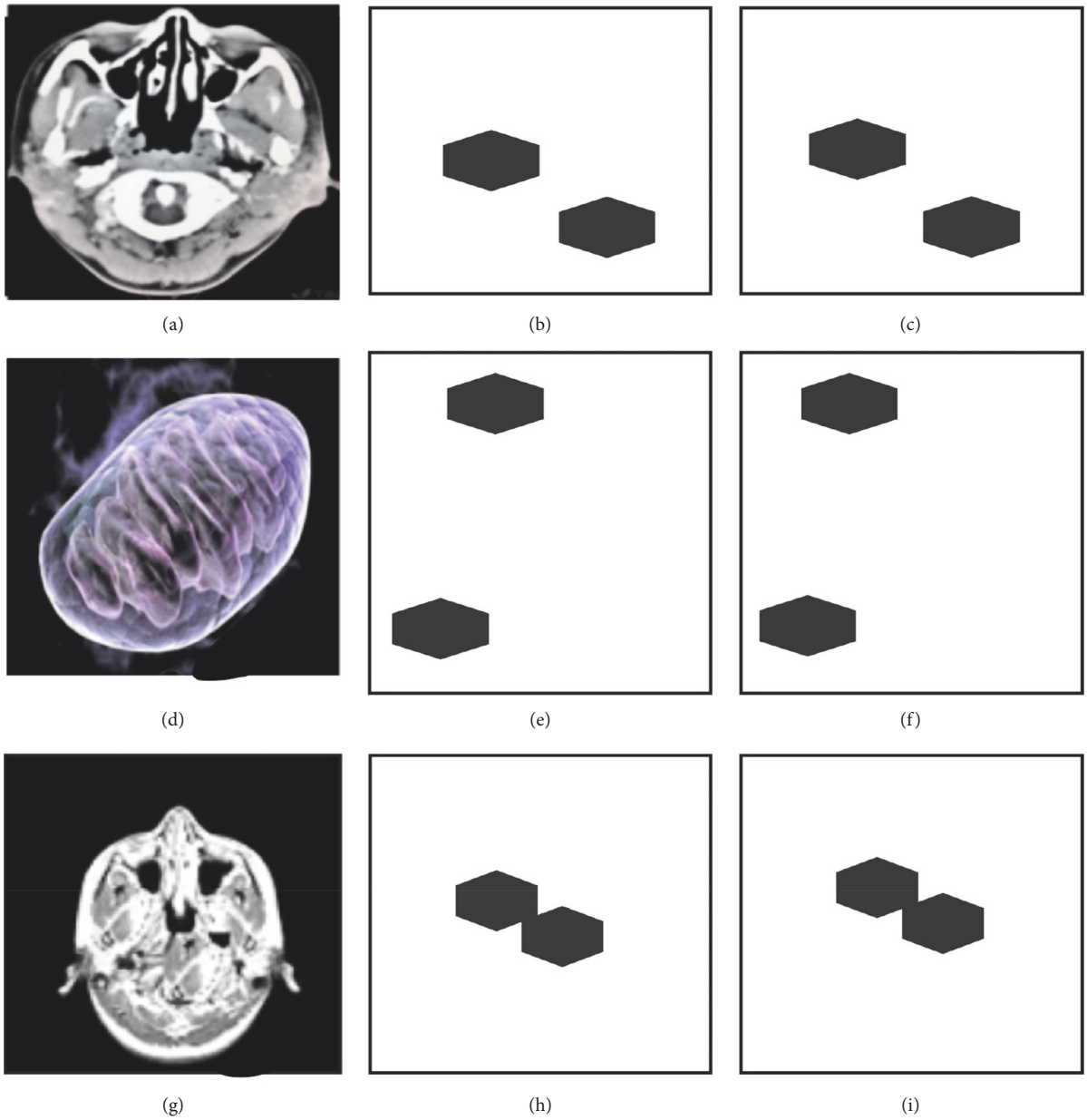

Figure 7: Comparison of the analysis results obtained based on the two algorithms. (a) Tampered image 1. (b) Result 1 obtained based on the neural network algorithm. (c) Result 1 obtained based on the algorithm proposed in this paper. (d) Tampered image 2. (e) Result 2 obtained based on the neural network algorithm. (f) Result 2 obtained based on the algorithm proposed in this paper. (g) Tampered image 3. (h) Result 3 obtained based on the neural network algorithm. (i) Result 3 obtained based on the algorithm proposed in this paper.

network algorithm can be replaced with horizontal-vertical restoration data, and this approach is effective. At the same time, the examples for the time pairs of the neural network algorithm and the algorithm put forward in this study are shown in Table 1, in which the split blocks are the rows of the sorted table. The number of blocks from the restored medical image 1 to the restored medical image 3 is 21060, 25281, and 11881, respectively. The block splitting features of the neural network algorithm are taken as the grayscale data of the medical image blocks, and the block splitting features of the algorithm proposed in this study are taken as the restoration data of the medical image blocks.

Table 2 shows that the rapid restoring algorithm of medical image based on the Bayesian personalized sorting algorithm is higher (97.4%) than conventional rule-based rapid image restoration methods in accuracy, and the proposed method time for rapid image restoration is shortened by 42.3%, which is rapid. Based on the experimental contrast of five thresholds (Table 3), rapid restoration threshold is set to 0.95. The results indicate that the algorithm has good balance and high accuracy, with a false positive rate of ≤26%, reported leak of ≤4.5%, false positive, and reported leak rates that remained low. Moreover, the threshold can also be adjusted as required

Table 2: Comparison of rapid image restoring algorithms.

Rapid image restoration method	Number of check out the actual image rapid restoring	Accuracy (%)	Image rapid restoring time
RATS	175	86.3	3′54″
Bayesian personalized sorting algorithm	193	97.6	2′18″

Table 3: Statistics of the image rapid restoration verification of the algorithm for the rapid restoration of 200 images.

Threshold	Number of checkout image rapid restoring	False positive	Reported leak	Accuracy (%)
1	187	3	13	98.5
0.94	196	5	8	97.5
0.84	216	23	14	89.2
0.74	215	46	28	78.4
0.62	257	92	36	64.2

by specific image rapid restoration to meet different needs of the image rapid restoration to realize the image rapid restoration. The false alarm rate and false alarm rate of medical image fast repair algorithm based on the Bayesian personalized sorting algorithm are 2.1% and 2.4%, respectively.

5. Conclusion

The application scope of the Bayesian personalized sorting algorithm in the field of image restoring is gradually expanding, and its corresponding effectiveness has also been recognized by all walks of life. In this study, by analyzing the problem of rapid restoration of medical images in different modalities, the data extraction of medical images can be better achieved using multi-modal data information, and an image with sound data information and rapid restoration can be obtained. Based on the Bayesian personalized sorting algorithm, a rapid restoring algorithm for medical images is proposed. The algorithm mainly realizes the preprocessing of the restored image through the segmentation of the initial image and the personalized sorting function. This algorithm can effectively reduce the complexity of image feature point extraction and feature matching, increase the anti-interference ability of the personalized sorting algorithm, and improve the robustness of the image to be restored. Finally, it can be known from experimental result analysis that the proposed algorithm proposed can achieve the three-dimensional reconstruction of medical images and convert them from two-dimensional structure to three-dimensional spatial reconstruction, thereby effectively improving the accuracy of clinical diagnosis and treatment. In short, as a powerful basis for improving the level of modern medical diagnosis, medical images make it possible to implement chemotherapy and surgery schemes with low risk and less trauma, which will receive more attention in the field of medical information research and computer image processing.

Data Availability

The data used to support the findings of this study are available from the corresponding author upon request.

Conflicts of Interest

The authors declare no conflicts of interest.

References

[1] D. M. Bappy and I. Jeon, "Combination of hybrid median filter and total variation minimisation for medical x-ray image restoration," *IET Image Processing*, vol. 10, no. 4, pp. 261–271, 2016.

[2] J. Miao, T. Z. Huang, X. Zhou, Y. Wang, and J. Liu, "Image segmentation based on an active contour model of partial image restoration with local cosine fitting energy," *Information Sciences*, vol. 447, pp. 52–71, 2018.

[3] A. A. Bini, "Image restoration via dost and total variation regularisation," *IET Image Processing*, vol. 13, no. 3, pp. 458–468, 2019.

[4] L. Chen, Y. Li, and T. Zeng, "Variational image restoration and segmentation with rician noise," *Journal of Scientific Computing*, vol. 78, no. 3, pp. 1329–1352, 2019.

[5] D. Q. Chen and Y. Zhou, "Wavelet frame based image restoration via combined sparsity and nonlocal prior of coefficients," *Journal of Scientific Computing*, vol. 66, no. 1, pp. 196–224, 2016.

[6] W. Hao and J. Li, "Alternating total variation and non-local total variation for fast compressed sensing magnetic resonance imaging," *Electronics Letters*, vol. 51, no. 22, pp. 1740–1742, 2015.

[7] J. Liu, J. Ma, Y. Zhang et al., "Discriminative feature representation to improve projection data inconsistency for low dose ct imaging," *IEEE Transactions on Medical Imaging*, vol. 36, no. 12, pp. 2499–2509, 2017.

[8] Y. Liu, X. Chen, R. K. Ward, and Z. J. Wang, "Medical image fusion via convolutional sparsity based morphological component analysis," *IEEE Signal Processing Letters*, vol. 26, no. 3, pp. 485–489, 2019.

[9] L. Lu and A. P. Harrison, "Deep medical image computing in preventive and precision medicine," *IEEE Multimedia*, vol. 25, no. 3, pp. 109–113, 2018.

[10] W. Jiang and Z. Yin, "Seeing the invisible in differential interference contrast microscopy images," *Medical Image Analysis*, vol. 34, pp. 65–81, 2016.

[11] Y. Du, J. L. Wang, and L. Lei, "Multi-objective scheduling of cloud manufacturing resources through the integration of Cat swarm optimization and Firefly algorithm," *Advances in Production Engineering & Management*, vol. 14, no. 3, pp. 333–342, 2019.

[12] M. Onoe, "Medical image processing," *Information Sciences*, vol. 175, no. 3, pp. 139-140, 2018.

[13] A. Qayyum, S. M. Anwar, M. Awais, and M. Majid, "Medical image retrieval using deep convolutional neural network," *Neurocomputing*, vol. 266, pp. 8–20, 2017.
[14] S. More, J. Singla, S. Verma, I. H. Ra, J. J. P. C. Rodrigues, and A. S. M. S. Hosen, "Security assured CNN-based model for reconstruction of medical images on the internet of healthcare things," *IEEE Access*, vol. 8, no. 99, pp. 126333–126346, 2020.
[15] P. J. Bardzinski, R. Krol, and L. Jurdziak, "Empirical model of discretized copper ore flow within the underground mine transport system," *International Journal of Simulation Modelling*, vol. 18, no. 2, pp. 279–289, 2019.
[16] G. D. Su, C. C. Chang, and C. C. Lin, "Effective self-recovery and tampering localization fragile watermarking for medical images," *IEEE Access*, vol. 8, no. 99, pp. 160840–160857, 2020.